

Benzoyl Phenyltelluride as Highly Reactive Visible-Light TERP-Reagent for Controlled Radical Polymerization

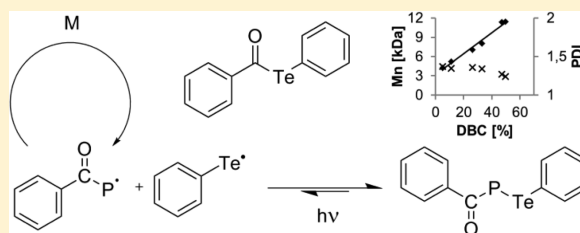
Stephan Benedikt,[†] Norbert Moszner,[‡] and Robert Liska^{*†}

[†]Institute of Applied Synthetic Chemistry, Division of Macromolecular Chemistry (part of the CD-Laboratory for Digital and Restorative Dentistry), Vienna University of Technology, Getreidemarkt 9/163/MC, 1060 Vienna, Austria

[‡]Ivoclar Vivadent AG (part of the CD-Laboratory for Digital and Restorative Dentistry), Bändererstrasse 2, FL-9494 Schaan, Liechtenstein

S Supporting Information

ABSTRACT: Benzoyl phenyltelluride (BPT) is a highly reactive TERP-reagent for visible-light-induced (400–500 nm) controlled radical polymerization. The compound can be easily prepared in one step from diphenyl ditelluride and benzoyl chloride. It shows a strong absorption at 407 nm that tails out to 473 nm and provides PDIs (1.2 to 1.3) among the lowest reported in literature for photoiniters in general, to which our compound was compared. PDIs obtained with BPT are much lower than those for benzyl dithiocarbamate (BDC) (1.7 to 1.8), which was used as a reference compound. Choice of BDC as reference is based on its property as UV-photoiniferter and on a similar initiation/control mechanism. However, BDC does not allow living radical polymerization under visible light. The newly discovered compound BPT provides best results with acrylamides and acrylates. Photoinitiation with styrene was ineffective, and reaction with methacrylates is not considered living.



INTRODUCTION

There are three classical ways to achieve controlled living radical polymerization (CRP): atom transfer radical polymerization (ATRP), which reacts according to an atom transfer mechanism,¹ nitroxide-mediated polymerization (NMP) with a dissociation–combination mechanism,² and reversible addition–fragmentation chain transfer (RAFT), which is based on degenerative transfer.³ These methods are well known and in use for various applications, such as drug delivery systems, synthesis of complex polymer architectures (e.g., star polymers), and others.^{4–6} The concentration of active radicals has to be kept low to avoid unwanted radical–radical recombination reactions to ensure a linear increase in the molecular weight with ongoing monomer double-bond conversion (DBC) and a narrow molecular weight distribution. While control is the main advantage, the main disadvantage is reduced reactivity and as a result a long reaction time (usually several hours). Furthermore, the classical living systems are usually thermally initiated, which provides less spatio and temporal control in comparison with photochemical systems. Photoiniters function as initiators that allow controlled living polymerization to provide better control.^{7,8} These systems are capable of behaving as photoinitiator, transfer agent, and polymerization control agent in one single compound and react based on a dissociation–combination mechanism. Applications for photoiniters include synthesis of complex polymer structures (e.g., surface grafted polymers), photolithography, photografting, and so on.^{9–12} In particular, for applications where a narrow polydispersity is beneficial, photoiniters

should be considered. One disadvantage, though, is the higher polydispersity (PDI) obtained by the use of photoiniters (1.5 for the best ones reported so far)¹³ in comparison with thermal control agents (1.1 to 1.4).⁸

To date, only a few compounds have been reported in literature, which shows the ability to function as photoiniters.^{7,14–18} Most of these compounds are based on a dithiocarbamate structure. To the best of our knowledge, these photoiniters are only active in the UV region, although many absorb up to 500–600 nm. This limits the use of photoiniters to applications where UV light is not considered problematic, but even there special light protection is usually required along with other problems that are to overcome.¹⁹

Recently new and alternative methods to achieve controlled radical polymerization were reported. Reversible chain transfer catalyzed polymerization and cobalt-mediated radical polymerization are only two of them.^{20,21} More important for our work is the organotellurium-mediated controlled radical polymerization (TERP).^{22,23} TERP has been established as a powerful method to achieve controlled radical polymerization, but most of the TERP-reagents still require additional thermal initiation or temperatures above room temperature. An exception is the photolabile TERP reagent (ethyl 2-phenyltellanyl-2-methylpropionate),²⁴ which allows reasonable molecular weight polymer with low polydispersity. On the basis of these prior good

Received: June 5, 2014

Revised: July 23, 2014

Published: August 14, 2014

results, we have chosen to study a benzoyl telluride compound, which cleaves to give a highly reactive benzoyl radical and also allows photoinduced TERP.

We describe the newly discovered polymerization control properties of the telluroorganic compound benzoyl phenyltelluride (**BPT**), which combines the positive characteristics of the already mentioned organotellurium compound ethyl 2-phenyltellanyl-2-methylpropionate with the reactivity of a benzoyl chromophore and compare it to the most relevant photoiniferter from literature benzyl dithiocarbamate (**BDC**).^{7,14–16} The comparison to a photoiniferter makes more sense than the comparison with other TERP reagents because TERP reagents behave very similar to photoiniferters when they are used as photoinitiator instead of thermal initiator.²⁴ This applies especially to the mechanism. While in thermally initiated TERP a degenerative transfer mechanism is exclusively responsible for the control abilities, in photoinduced TERP, a dissociation–combination is assumed to also play an important role, although degenerative transfer still occurs as a competing reaction.²⁵ This is also the case for photoiniferters, even though the degenerative transfer is less important. It is worth mentioning that a similar compound (benzoyl methyltelluride) to our **BPT** has already been described in literature as a thermal TERP-reagent, but this compound showed poor control abilities because of the high C–Te-bond dissociation energy, which should be lower in our case due to an aryl substituent on the Te atom.²⁶ We will show that **BPT** can be used as control agent for acrylates (ACs) and acrylamides (AMs) in the visible light (400–500 nm) region. The ability of **BPT** to control the polymerization has been confirmed by steady-state polymerization experiments, which include measurements of the polydispersity and the combination of molecular weight and DBC, respectively. While rate constants for reactions of dithiocarbamyl radicals were reported in literature,²⁷ no constants for photoinduced reactions of TERP reagents have been reported yet. Therefore, the comparison of control abilities will be done on the basis of achievable PDIs. A polymerization mechanism based on literature is proposed; photo-DSC and UV–vis measurements are provided for comparison with other photoinitiating systems.

EXPERIMENTAL SECTION

Materials. The monomers styrene (St), *n*-butyl acrylate (BA), *n*-butyl methacrylate (BMA), and 4-acryloylmorpholine (NAM) and the photoiniferters/photoinitiators benzyl dithiocarbamate (**BDC**), monoacylphosphinoxide (**MAPO**) (diphenyl(2,4,6-trimethylbenzoyl)-phosphine oxide), camphorquinone (**CQ**), and ethyl 4-(dimethylamino)-benzoate (**DMAB**) are commercially available (Aldrich) and were used in the highest purities available. Benzoyl phenyltelluride (**BPT**) was synthesized according to a slightly modified synthetic procedure described in literature.²⁸

Synthesis of Benzoyl Phenyltelluride (BPT). All synthesis was performed under light protection in an orange light lab, which excludes wavelengths below 520 nm. The following procedure is slightly modified from that of Gardner et al.²⁸ Diphenyl ditelluride (3.23 mmol, 1.32 g) was dissolved in a mixture of toluene and ethanol (5 mL, 25/75 v/v) and heated to reflux. To this solution NaBH₄ (5.17 mmol, 0.20 g) dissolved in 1N NaOH (4.4 mL) was added dropwise. During the addition, there appeared a strong formation of H₂, and the solution became colorless. Then, benzoyl chloride (7.75 mmol, 1.09 g, 0.89 mL) was added in one portion, and the warm reaction mixture was stirred for another 5 min. Afterward, 25 mL of water was added, and the resulting mixture was extracted with diethyl ether. The combined organic phase was dried over anhydrous Na₂SO₄, and after removal of the solvent the crude product was purified via liquid

chromatography (PE/Et₂O 20:1, silica gel) to yield 1.48 g (74% of theory) of pure **BPT** as a bright yellow powder. m.p.: 70–72 °C. GC–MS (THF, EI, *m/z*): 311.96 (M); 282.00; 206.99; 154.10; 105.03; 77.06. ¹H NMR (CD₂Cl₂, δ): 7.75–7.49 (m, 5H, CO–C₆H₅); 7.48–7.20 (m, 5H, Te–C₆H₅). ¹³C NMR (CD₂Cl₂, δ): 143.3; 141.1; 134.5; 129.9; 129.6; 129.3; 127.3; 125.7. IR (ATR, cm⁻¹): 1663.47 ν(C=O).

UV–vis Measurements. UV–vis measurements were carried out on a Shimadzu UV-1800 spectrophotometer using quartz cuvettes with 10 mm thickness. The photoiniferter samples were dissolved in CH₂Cl₂ with a concentration of 1 × 10⁻³ mol L⁻¹ for **BDC**, **BPT**, and **MAPO** and with 1 × 10⁻² mol L⁻¹ for **CQ** and measured in the dark.

Kinetic Studies. The photopolymerization of the four different monomers (BA, BMA, St, NAM) was carried out in a photoreactor (Figure S1 in the Supporting Information). The reactor was filled to a height of ~25 mm with monomer formulation (monomer + **BPT**/**BDC**), which was degassed with argon. For irradiation an OmniCure 2000 (Lumen Dynamic), mercury lamp with a filter excluding all but 400–500 nm was used. The effective irradiation intensity was adjusted to the reactivity of the monomer (0.07 W cm⁻² on the surface of the formulation for BA, BMA, and St and 0.03 W cm⁻² on the surface for NAM). For the more reactive monomers, a lower effective irradiation intensity and photoiniferter/TERP-reagent to monomer molar ratio was chosen (BA: 1:200, BMA: 1:100, St: 1:100, NAM: 1:500) to make sure the polymerization would be slow enough to take samples. These samples were taken with a syringe over the side joint of the reactor. Typical sample size was 0.05 mL, of which 10 mg was used for GPC analysis and the rest of ~40–50 mg was used for ¹H NMR spectroscopy.

For determination of the number-average molecular weight (*M_n*) and the polydispersity index (PDI), a Waters 717plus GPC with three columns (Styragel HR 0.5 THF, Styragel HR 3 THF, and Styragel HR 4 THF) and a Waters 2410 refractive index detector were used. The eluent was THF with a flow rate of 1.0 mL min⁻¹, and the temperature was set to 40 °C. For calibration, polystyrene standards were used, which offer a molecular weight resolving range of 10² to 10⁶ g/mol.

A Bruker AC-E-200 FT-NMR-spectrometer was used for the samples taken from the photoreactor to determine the monomer DBC. The solvent was deuterated chloroform (CDCl₃) with a degree of deuteration ≥99.8% D. Out of these spectra, the double-bond conversion was calculated by comparing the integrals of the monomer specific double bonds to the combined integrals of the side chains of monomer and polymer.

Photo-DSC Measurements. Photo-DSC analysis was done on a Netzsch DSC 204 F1 using an OmniCure 2000 (Lumen Dynamic) mercury lamp light source equipped with a built-in 400–500 nm filter. The lamp was calibrated with an OmniCure R2000 radiometer to an effective irradiation intensity of 3.00 W cm⁻². The measurements were done with 10 ± 1 mg of monomer formulation, which consisted of photoinitiator/CRP-reagent and NAM in a molar ratio of 1:500 (0.3 to 0.5 wt %). As a result from the measurements, the time until the maximum heat of polymerization (*t_{max}*) is reached can be obtained directly. Also, the time until 95% of the maximum DBC (*t_{95%}*) can be directly acquired through integration of the resulting curves. However, the rate of polymerization (*R_p*) and the DBC of the monomer need to be calculated according to eqs 1 and 2

$$R_p = \frac{\Delta H_{\max} \cdot \rho}{\Delta H_0 \cdot M_w} \quad (1)$$

$$\text{DBC} = \frac{A}{\Delta H_0} \cdot 100 \quad (2)$$

Herein ΔH_{\max} is the maximum heat of polymerization, ΔH_0 (NAM: 513.57 J g⁻¹)²⁹ is the theoretical heat of polymerization, ρ (NAM: 1114 g L⁻¹)²⁹ is the density of the formulation, M_w is the molecular weight, and A is the integrated area of the DSC plot. All of these numbers are referring to the monomer.

RESULTS AND DISCUSSION

UV–vis Spectroscopy. The UV–vis spectrum (Figure 1) of the tellurium compound **BPT** is compared with the spectrum of the dithiocarbamate **BDC** and a classical Type I (**MAPO**) and Type II (**CQ**) photoinitiator.

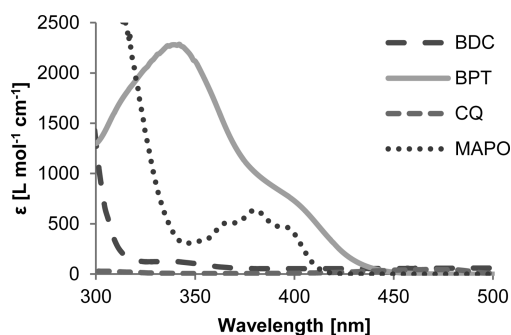


Figure 1. UV–vis-absorption spectra of the photoinitiators/photoinitiators **BDC**, **BPT**, **MAPO**, and **CQ** (1×10^{-3} mol L $^{-1}$ for **BDC**, **BPT**, and **MAPO** and 1×10^{-2} mol L $^{-1}$ for **CQ** in CH $_2$ Cl $_2$).

The telluride **BPT** has a maximum of 339 nm in the absorption spectrum, which most likely marks the $n-\sigma^*$ transition of the compound. This was already shown in literature for telluriumorganic compounds by using time-dependent DFT calculations.²⁴ In this band, a significant shoulder appears at 407 nm that tails out until 473 nm, which can be assigned to the $n-\pi^*$ transition of the carbonyl moiety. This is in good accordance with other Ar–CO–X systems like acylphosphinioxides (e.g., **MAPO**, $\lambda = 380$ nm) and acyl germanium compounds (e.g., benzoyltrimethylgermane, $\lambda = 412$ nm).³⁰ The strong shift of the $n-\pi^*$ transition compared with the classical benzoyl chromophore ($n-\pi^* \sim 350-360$ nm) can be explained by the overlap of the d orbitals of P, Ge, or Te with the π^* orbital of the C=O group, thus reducing the necessary energy for the $n-\pi^*$ transition.

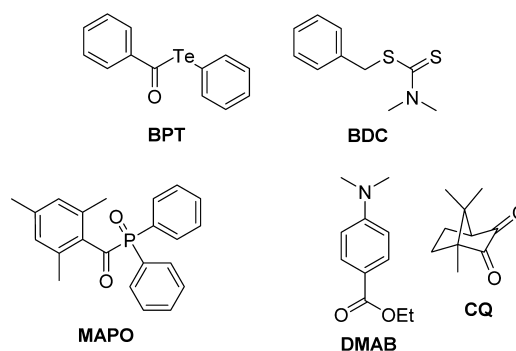
BDC has its maximum absorption (belonging to the $n-\pi^*$ transition of the carbamate moiety) at 335 nm.^{31,32} Because of the high conjugation of this functional group, the peak tails out far into the visible region even above 500 nm. The extinction coefficient is 50 L mol $^{-1}$ cm $^{-1}$, which is very low but still in the same range of **CQ**.

The classical type-II photoinitiator **CQ** has its absorption maximum at 468 nm. The long wavelength of the $n-\pi^*$ transition can be explained by the angle between the two carbonyl groups (Scheme 1).³³

Controlled Living Radical Photopolymerization. The living character of a polymerization can be proven with studies of the polymerization kinetics (Figure 2).³⁴ If the polymerization occurs according to a living mechanism, the molecular weight increases in a linear relationship with the DBC of the monomer. Also, the PDI should be significantly below 1.5 because the control agent should theoretically provide a homogeneous chain length. In the case of a free radical polymerization, the overall number-average molecular weight (M_n) will decrease before the gel point is reached. Moreover, because of termination and unwanted transfer reactions, the PDI will usually be above 1.5.

The living character of the reference **BDC** for a polymerization carried out with UV light has already been shown in literature.¹³ The typical PDI for that compound as photoinitiator for the bulk polymerization of MMA is around 1.7 to

Scheme 1. Photoinitiator/CRP Systems Tested in the Present Paper



1.8 over 50% conversion. In that paper, also a linear correlation between increasing molecular weight and DBC has been proven.

In the present study, the experiments for the determination of the polymerization kinetics were carried out in a photoreactor with a 400–500 nm light source and four different classes of monomers (St, BMA, BA, NAM). The molar concentration of photoinitiator/TERP-reagent in the monomer varies between 1:100 and 1:500 (0.3 to 2.2 wt %) and was adjusted to the reactivity of the monomer. For both the reference **BDC** and the tellurium compound **BPT**, M_n versus DBC plots from data of ^1H NMR-spectroscopy and GPC measurements were made. Additionally, the PDIs of the synthesized polymers were measured.

In general, styrene photoinitiation with both **BDC** and **BPT** was ineffective because styrene is more likely to quench the initiator than to propagate under these conditions. By comparison, TERP-reagents have been previously shown to moderate styrene propagation under thermal initiation conditions (Yamago 2013).³⁵ The methacrylate BMA could be polymerized with both **BDC** and **BPT** but not in a living radical polymerization, and the rate for the reference **BDC** was very low (Figures S2 and S3 in the Supporting Information). This is in good accordance with literature, which highlights the important role of dimethyl ditelluride for the controlled TERP polymerization of methacrylates.³⁶ The monomers BA and NAM both met the criteria for a living radical polymerization with our compound **BPT** (Figure 2). It has to be noted that NAM was only polymerized to a DBC of $\sim 20\%$ with both photoinitiators due to its high viscosity, which made it impossible to take samples from the photoreactor at higher DBCs.

The increase in the PDI for NAM with **BPT** in the beginning can be explained by termination reactions, which still appear in this early phase of the polymerization.

At conversions as low as 4%, M_n has values around 4 to 5 kDa for both BA and NAM polymerized with the tellurium compound **BPT**. M_n increases linearly with DBC to values around 11 kDa. The deviation of the best-fit line from the origin is due to radical recombination reactions, which still appear in the early stage of the reaction.¹⁸ This causes an initial steep increase in molecular weight as the initiator is consumed, followed by a less steep but linear propagation phase. All of this is in good accordance with other photoinitiator studies found in literature.¹³ The PDIs are significantly below 1.5 and are as low as 1.2 for BA over 50% DBC and 1.3 for NAM over 50% DBC (PDI over 50% DBC for **BDC** according to literature: 1.7 to

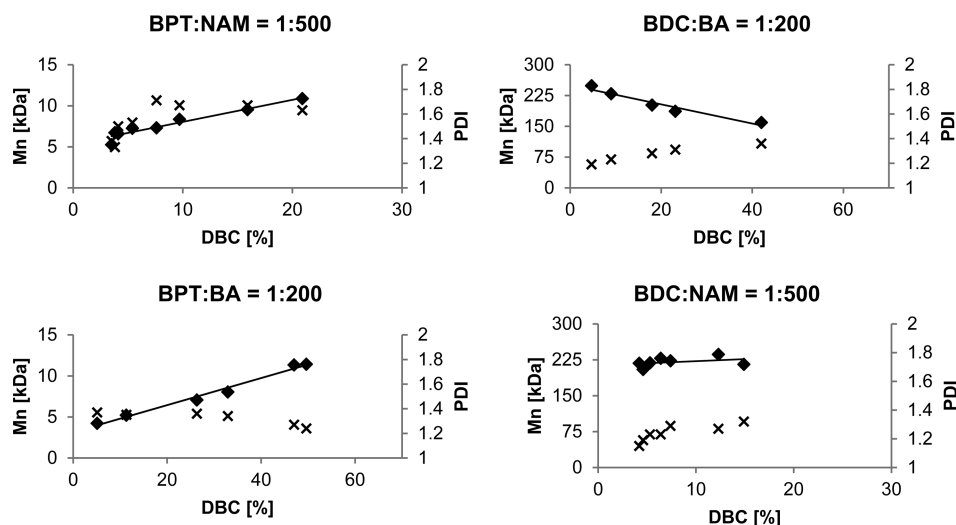


Figure 2. Number-average molecular weight M_n (diamonds) and PDI (crosses) versus double-bond conversion (DBC) plots for BDC and BPT with BA and NAM in bulk determined with photoreactor experiments.

Table 1. UV-vis Data^a and Results of the Photo-DSC Measurement with CRP-Reagent/Photoinitiator in NAM with a Molar Ratio of 1:500 Each

	R_p [10^{-3} mol L ⁻¹ s ⁻¹]	DBC [%]	t_{max} [s]	$t_{95\%}$ [s]	λ_{max} [nm]	ϵ [L mol ⁻¹ cm ⁻¹]
BDC	15.9	40	53.5	257	335	126
BPT	14.0	29	33.0	180	407 ^b	595
MAPO	665.2	89	8.0	22	380	636
CQ/DMAB	281.0	80	14.1	34	468	44

^a 1×10^{-3} mol L⁻¹ for BDC, BPT, and MAPO and 1×10^{-2} mol L⁻¹ for CQ in CH₂Cl₂. ^bAbsorption at the shoulder of the UV-vis spectrum determined by peak deconvolution, marking the $n-\pi^*$ transition of the carbonyl group

1.8).¹³ This fact is especially remarkable because the best photoiniferter system so far (benzyl 9*H*-carbazole-9-carbodi-thioate) can only reach a PDI of 1.5 over 40% conversion.¹³

In contrast with BPT, the reference BDC was not suitable for living polymerization under visible light for any tested monomer. Even though the PDIs were below 2 for BA and NAM, M_n does not increase linearly for either monomer.

Photoreactivity Determined by Photo-DSC. The reactivity of the telluride BPT was compared with the reactivity of the reference dithiocarbamate BDC. The comparison was done only for acrylamides because the reactivity of butyl acrylate was too low to produce significant and accurate results with photo-DSC. In general, the reactivity of photoiniferters is lower than the reactivity of photoinitiators, which can be explained by the reaction mechanism. While photoinitiators produce radicals, which directly induce radical chain growth, the use of photoiniferters leads to the formation of so-called dormant species during the polymerization reaction. These species have to be reactivated by light, which leads to a significant decline of the reaction rate. Of course, this is a generalization, and it also has to be mentioned that other effects like quantum yields of the compounds play an important role as well. Nevertheless, classical photoinitiator systems, which initiate in the visible-light range (MAPO and CQ/DMAB) were measured (Table 1 and Figure 3), too, to compare the CRP-reagents among commercially used photochemical polymerization systems.

As expected, the reactivity (expressed by R_p , t_{max} and $t_{95\%}$) and the DBC of the classical free radical photoinitiator systems MAPO and CQ/DMAB are significantly higher than the values for the CRP-reagents. The photoiniferters BDC and BPT are

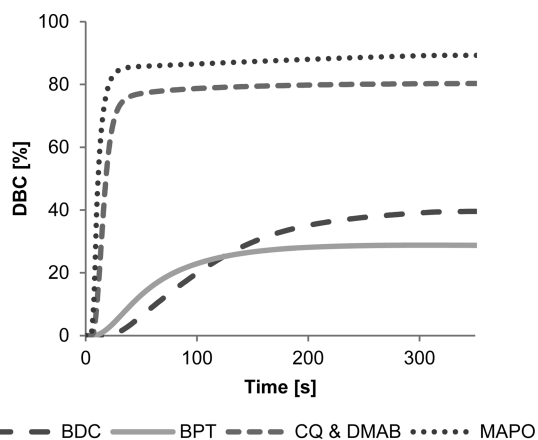
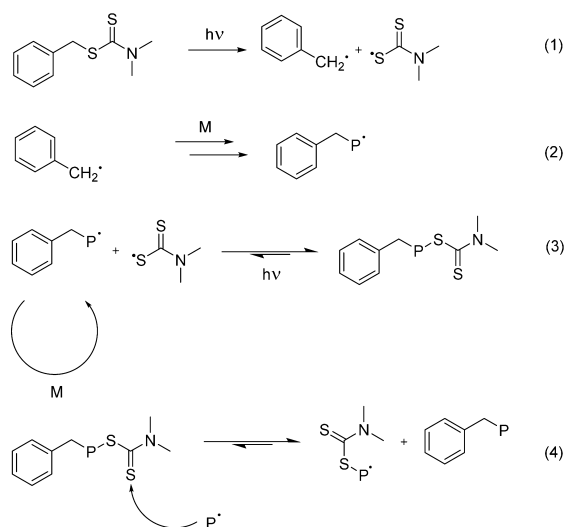
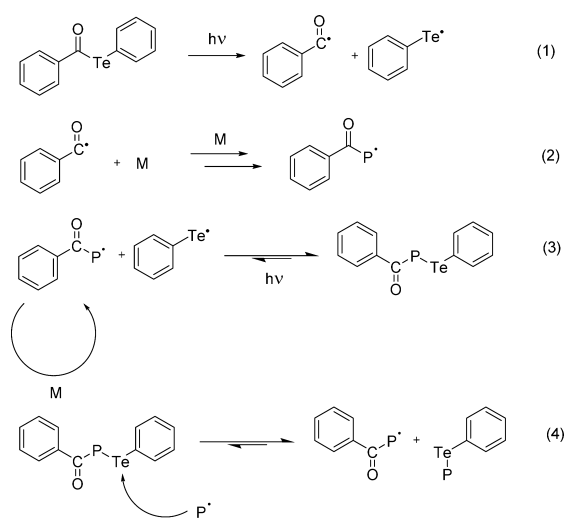


Figure 3. Double-bond conversion DBC [%] versus time [s] for the CRP reagents BDC and BPT and for the photoinitiator systems MAPO and CQ/DMAB in NAM with a molar ratio of 1:500 each (0.3, 0.4, 0.5, and 0.5 wt %, respectively).

both in a similar range of reactivity. The rate of polymerization R_p is approximately the same (14.0×10^{-3} mol L⁻¹ s⁻¹ for BPT and 15.9×10^{-3} mol L⁻¹ s⁻¹ for BDC), but the time until the maximum heat of polymerization t_{max} is reached and the time until 95% of the polymerization reaction is completed $t_{95\%}$ are significantly lower for our BPT. The reason for that might be the formation of a highly reactive benzoyl radical in the case of BPT (which is also the main difference to the photoinducible TERP reagent ethyl 2-phenyltellanyl-2-methylpropionate) instead of a benzyl radical as for BDC,^{8,13} which makes the initiation step very efficient (Schemes 2 and 3, line 2). The

Scheme 2. Mechanism for the Living Radical Polymerization with BDC as Photoiniferter⁸**Scheme 3. Proposed Living Radical Polymerization Mechanism with BPT as TERP-Reagent²⁴**

BDC is, with ~30% for BPT and ~40% for BDC for both systems, relatively low. The higher DBC for the reference BDC can be explained by the noncontrolled polymerization mechanism.

Higher DBC (>50%) for BPT can be achieved by using higher photoiniferter concentrations, which necessitates longer polymerization times or a higher light intensity (Figure S4 in the Supporting Information). However, the tested concentration was chosen because it provides comparable results for every tested system and is also consistent with the concentrations used for polymerization kinetic studies.

In general, the fact that the reference BDC is slightly less reactive does not come as a surprise. Literature already suggests that BDC would need UV light for reinitiation⁸ (Scheme 2, line 3) or at least UV light would make this reinitiation much more efficient.¹³

Poor visible-light efficiency of BDC is explained by poor overlap with the $n-\pi^*$ transition, which has its maximum in the UV region. It thus requires UV light for efficient cleavage of the C–S bond between polymer and chain-transfer agent. It

can be assumed that the absorption in the visible-light region for the reagent BDC is similar to the resulting dormant species. Therefore, cleavage can take place but is very inefficient, which results in no control of the polymerization. In contrast, it can be expected from the dormant species of our BPT to still efficiently cleave in the visible light area, which is in good accordance with literature.²⁴ It is also worth mentioning that a degenerative transfer mechanism may compete with the described mechanism (Scheme 2, line 4), therefore reducing the reactivity of BDC, but for the control of polymerization, the dissociation–combination mechanism plays the main role.¹³

The tellurium compound BPT reacts via a similar mechanism, which is already proposed in literature for another telluroorganic compound.²⁴ The adapted mechanism for the specific photoiniferter is shown in Scheme 3.

The cleavage of the C–Te-bond (Scheme 3, Line 3) requires less energy (absorption above 400 nm) and is therefore still efficient under the influence of visible light, which was already shown in literature for TERPs.^{23,35} It has to be noted that also here degenerative transfer (Scheme 3, line 4) may compete with the dissociation–combination mechanism (Scheme 3, line 3) and may even be very important for polymerization control. However, while degenerative transfer is the major mechanism for thermally initiated TERP, for photoinduced TERP, the dissociation–combination also plays a major role.^{24,25} For sure, the exact mechanism needs to be elucidated in future work, but the proposed mechanism based on literature gives us a first plausible explanation.

CONCLUSIONS

We have shown that the telluroorganic compound BPT is a suitable polymerization control agent for acrylates and acrylamides, yielding polydispersities as low as 1.2 to 1.3. To our best knowledge, BPT leads to lower polydispersities than it was reported in literature for photoiniferters so far. The most important benefit of BPT, though, can be found in the ability to carry out controlled radical polymerization at room temperature with a visible light (400–500 nm) radiation source. The reference BDC also has some potential but needs UV light for its living radical polymerization mechanism. Explanation can be given by the UV–vis spectrum, in general, and the $n-\pi^*$ transition (335 nm for BDC and 407 nm for BPT) of the two compared compounds in particular. The subsequently formed tellurium dormant species was still active under visible-light irradiation. The high reactivity of the tellurium compound BPT compared with the reference BDC has been shown by photo-DSC experiments and can be attributed to the highly reactive benzoyl radical. In conclusion, BPT is highly suitable for photopolymerizations, where a narrow molecular weight distribution is mandatory and visible light is preferred.

ASSOCIATED CONTENT

Supporting Information

Figure S1: Photoreactor. Figures S2 and S3: Polymerization kinetics of BMA with BPT and BDC. Figure S4: Photo-DSC measurements of NAM with BPT in different concentrations and with different light intensities. This material is available free of charge via the Internet at <http://pubs.acs.org>.

AUTHOR INFORMATION

Corresponding Author

*E-mail: Robert.Liska@tuwien.ac.at. Tel: +43-1-58801-163614. Fax: +43-1-58801-16299.

Notes

The authors declare no competing financial interest.

ACKNOWLEDGMENTS

We thank the Christian Doppler society for financial support.

REFERENCES

- (1) Matyjaszewski, K.; Xia, J. *Chem. Rev.* **2001**, *101*, 2921–2990.
- (2) Hawker, C. J.; Bosman, A. W.; Harth, E. *Chem. Rev.* **2001**, *101*, 3661–3688.
- (3) Chiefari, J.; Chong, Y. K.; Ercole, F.; Krstina, J.; Jeffery, J.; Le, T. P. T.; Mayadunne, R. T. A.; Meijs, G. F.; Moad, C. L.; Moad, G.; Rizzardo, E.; Thang, S. H. *Macromolecules* **1998**, *31*, 5559–5562.
- (4) Kong, H.; Gao, C.; Yan, D. *J. Am. Chem. Soc.* **2004**, *126*, 412–413.
- (5) Bosman, A. W.; Vestberg, R.; Heumann, A.; Frechet, J. M. J.; Hawker, C. J. *J. Am. Chem. Soc.* **2003**, *125*, 715–728.
- (6) Bajpai, A. K.; Shukla, S. K.; Bhanu, S.; Kankane, S. *Prog. Polym. Sci.* **2008**, *33*, 1088–1118.
- (7) Otsu, T.; Yoshida, M. *Makromol. Chem., Rapid Commun.* **1982**, *3*, 127–32.
- (8) Otsu, T. *J. Polym. Sci., Part A: Polym. Chem.* **2000**, *38*, 2121–2136.
- (9) Rohr, T.; Hilder, E. F.; Donovan, J. J.; Svec, F.; Frechet, J. M. J. *Macromolecules* **2003**, *36*, 1677–1684.
- (10) Choi, S.-J.; Yoo, P. J.; Baek, S. J.; Kim, T. W.; Lee, H. H. *J. Am. Chem. Soc.* **2004**, *126*, 7744–7745.
- (11) de Boer, B.; Simon, H. K.; Werts, M. P. L.; van der Vegte, E. W.; Hadziioannou, G. *Macromolecules* **2000**, *33*, 349–356.
- (12) Schmelmer, U.; Paul, A.; Kueller, A.; Steenackers, M.; Ulman, A.; Grunze, M.; Goelzhaeuser, A.; Jordan, R. *Small* **2007**, *3*, 459–465.
- (13) Lalevee, J.; Blanchard, N.; El-Roz, M.; Allonas, X.; Fouassier, J. P. *Macromolecules* **2008**, *41*, 2347–2352.
- (14) Kuriyama, A.; Otsu, T. *Polym. J. (Tokyo, Jpn.)* **1984**, *16*, 511–14.
- (15) Otsu, T.; Tazaki, T. *Polym. Bull. (Berlin)* **1986**, *16*, 277–84.
- (16) Bertin, D.; Boutevin, B.; Gramain, P.; Fabre, J.-M.; Montginoul, C. *Eur. Polym. J.* **1998**, *34*, 85–90.
- (17) Lalevee, J.; Allonas, X.; Fouassier, J. P. *Macromolecules* **2006**, *39*, 8216–8218.
- (18) Lalevee, J.; El-Roz, M.; Allonas, X.; Fouassier, J. P. *J. Polym. Sci., Part A: Polym. Chem.* **2007**, *45*, 2436–2442.
- (19) Bromme, T.; Moebius, J.; Schafer, S.; Schmitz, C.; Strehmel, B. *Eur. Coat. J.* **2012**, *20–21* (24–26), 27.
- (20) Goto, A.; Tsujii, Y.; Fukuda, T. *Polymer* **2008**, *49*, 5177–5185.
- (21) Debuigne, A.; Poli, R.; Jerome, C.; Jerome, R.; Detrembleur, C. *Prog. Polym. Sci.* **2009**, *34*, 211–239.
- (22) Yamago, S. *Chem. Rev.* **2009**, *109*, 5051–5068.
- (23) Yamago, S.; Nakamura, Y. *Polymer* **2013**, *54*, 981–994.
- (24) Yamago, S.; Ukai, Y.; Matsumoto, A.; Nakamura, Y. *J. Am. Chem. Soc.* **2009**, *131*, 2100–2101.
- (25) Nakamura, Y.; Kitada, Y.; Kobayashi, Y.; Ray, B.; Yamago, S. *Macromolecules* **2011**, *44*, 8388–8397.
- (26) Yamago, S.; Iida, K.; Yoshida, J. *J. Am. Chem. Soc.* **2002**, *124*, 2874–2875.
- (27) Fouassier, J.-P.; Lalevee, J. 2012.
- (28) Gardner, S. A.; Gysling, H. J. *J. Organomet. Chem.* **1980**, *197*, 111–122.
- (29) Gugg, A. *Development of Monomers and Additives for Advanced Dental Formulations*. Vienna University of Technology, Vienna, AT, 2011.
- (30) Ganster, B.; Fischer, U. K.; Moszner, N.; Liska, R. *Macromolecules* **2008**, *41*, 2394–2400.
- (31) Rang, K.; Sandstrom, J. *J. Chem. Soc., Perkin Trans. 2* **1999**, 827–832.
- (32) Petrov, I.; Simonovska, B. *J. Mol. Struct.* **1986**, *142*, 167–70.
- (33) Arnett, J. F.; Newkome, G.; Mattice, W. L.; McGlynn, S. P. *J. Am. Chem. Soc.* **1974**, *96*, 4385–92.

(34) Qiu, J.; Charleux, B.; Matyjaszewski, K. *Prog. Polym. Sci.* **2001**, *26*, 2083–2134.

(35) Nakamura, Y.; Yamago, S. *Beilstein J. Org. Chem.* **2013**, *9*, 1607–1612.

(36) Kwak, Y.; Tezuka, M.; Goto, A.; Fukuda, T.; Yamago, S. *Macromolecules* **2007**, *40*, 1881–1885.